

# CFD TESTS OF THE EXHAUST SYSTEM OF A SPORTS MOTORCYCLE

**Marcin Tkaczyk**

*Wroclaw University of Science and Technology  
Division of Automotives Engineering  
Braci Gierymskich Street 164, 51-640 Wroclaw, Poland  
tel.: +48 71 3477918, fax: +48 71 3477918  
e-mail: marcin.tkaczyk@pwr.edu.pl*

## **Abstract**

*The content of this article describes the area of the operation of speedway racing motorcycles, it reflects the specific use, and thus, the special requirements placed on the internal combustion engines used there. Then, a research tool is presented in the form of Computational Fluid Dynamics methods. The article presents basic equations as a base for software, and emphasizes the essence and necessity of adequate selection of turbulence models. Presentation of the work tool is crowned with a brief description of the application in the form of Ansys numerical analysis software and a specific place and possibilities of its application. The practical part describes the work carried out during the tests of a GM 500 type combustion engine and attempts to compare two types of exhaust systems whose advantages and disadvantages in analytical calculations are difficult to determine, whereas CFD tests accurately represent pressure fields, velocities and the most important parameter in the form of resistance of the exhaust system. The article is crowned with the results of tests enabling determination and selection of the exhaust system with lower flow resistance and recommendations adjusting the exhaust system to a specific engine.*

**Keywords:** CFD, speedway, spark ignition engine

## **1. Introduction**

Motorcycle speedway (commonly referred to as “speedway”) is one of the motorsport disciplines. Usually, four competitors race on special motorcycles along an oval-shaped track in an anti-clockwise direction for four laps. The sport is characterized by the fact that the track has a loose surface and that the motorcycles have no gearbox or brakes. Around the world, it is known as speedway. The Polish name, “żużel”, derives from the area on which the competition was once held, i.e. the black slag surface. Currently, mixtures of syenite or granite are used.

In a race, there are four competitors, who make four laps from a standing start, i.e. the vehicles are stationary before the start. A competition usually consists of 15 runs for team matches and 20 for grand prix [5].

This article contains content describing project work carried out with CFD support; therefore, a brief description of the issue is necessary.

Computational Fluid Dynamics (CFD) is a branch of fluid mechanics that uses numerical analysis and data structures to solve and analyse problems that involve fluid flows. It is used to approximate the distribution of velocity, pressure, temperature and other parameters in the flow, by discretizing and solving partial differential equations describing the flow. Modern CFD programs allow solving flows with regard to viscosity and compressibility, multiphase flows, flows in which chemical reactions or combustion processes occur, flows through porous structures, and flows in which the medium is Newtonian or non-Newtonian fluid. It is also possible to simulate a Fluid Structure Interaction.

Currently, we can find a wide range of software that allows modelling flows. These include ANSYS, FIDAP, FLOW3D, etc. They all contain extensive user interfaces, with which it is possible to set geometry and flow parameters and graphical visualization of calculations. The workflow of such computer programs can be presented as follows [2]:

- preparation for calculations – formulation of a mathematical model, generation of a computational grid, data input (so-called pre-processing),
- calculations – solving the problem using a solver (so-called solving),
- development of calculation results (so-called post processing).

In the first stage, you must specify the geometry of the calculated area, and then generate a grid covering this area. The next step is to determine the boundary conditions and to give physical parameters of the factor flowing through this area, i.e. density, viscosity, specific heat or thermal conductivity coefficient. Before starting calculations, one must determine the type of model that will be used to model the tested flow, i.e. whether the flow is laminar or turbulent, whether compressible or incompressible, whether it is to take into account thermal conductivity or not.

The equations of fluid motion are non-linear, and therefore these equations can only be solved in a few special cases. Therefore, numerical equations are solved in an approximate way by discretization. The result of discretizing is the replacement of differential equations by a system of algebraic equations. This is done by using numerical grids. In numerical fluid mechanics, the most commonly used discretization methods are: Finite Volume Method, Finite Element Method, Finite Difference Method.

Finite difference method is one of the oldest methods of solving differential equations. It uses the differential form of Navier-Stokes equations for the analysis of flow phenomena. It is based on the separation of nodes in the analysed area in which the derivative is transformed in differential equations to finite differences, i.e. the differential equations are approximated to the form of the difference quotients. Due to its significant limitations, this method is currently not used in computer systems.

Currently, one of the most popular methods of discretization is the finite volume method. It involves the transformation of the geometric model of the flow region from the continuous form to the discrete form as cells with a certain volume, also called the control volume. Digitized geometry is a grid in which computing nodes can be placed in the geometric centre of the cell. The transformation of differential equations into algebraic equations is based on the integration of these equations within the boundaries of each finite volume. The advantage of this method is great freedom of shaping control areas, which makes it easy to generate appropriate equations determining the nodal values of the function sought.

## **2. Description of the practical part**

This article reflects the course and results of research on two exhaust systems designed for use in the GM500 internal combustion engine used in speedway motorcycles. Both exhaust systems have very similar shape and dimensions; they are approved for use in all types of speedway trainings and competitions. The difference between the systems lies in the method of solving the shape of the so-called “elbow” or element enabling the change of the direction of exhaust gas flow from the engine. The outlet of the exhaust gases from the engine head is directed towards the ground but must be directed in the opposite direction and this task is currently carried out in two ways: the first one is to change the outlet gas flow account by using a single arc with an angle of 90°, while the second one consists of using two 45° arches connected by a straight section.

The research and research results as well as the evaluation of solutions are described below. Both exhaust systems were evaluated using the flow loss criterion, while the size of the active cross-sectional area of the pipe was analysed. The cross-section is considered to be the area that is occupied by velocity vectors in the direction of flow, in addition the size of velocity vectors is also important and should be as much as the value of the mean flow velocity.

### **2.1. Flow test**

The construction of the numerical model included:

- mapping of interior elements of the intake system,
- transformation of geometry to a numerical form,
- discretization of computing space,
- assignment of boundary conditions,
- selection of the description of physical phenomena,
- selection of the application method of differential equations,
- calculations,
- visualization of calculation results.

The above-mentioned methodology of operation, described in detail in [6] works, applied to both types of exhaust system.

Realization of points regarding: mapping of intake system elements, transformation of geometry to numerical form, discretization of computational space, assignment of boundary conditions, selection of physical phenomena description, choice of application of differential equations, calculations, belongs to the clichéd tasks carried out in the research methodology and described in detail in the works [author's]. However, the individual issue is the adoption of boundary conditions for this type of CFD application, which is why the boundary conditions for calculating the flow through the exhaust system of the GM500 combustion engine are described below.

### *Selection of boundary conditions*

The average velocity of exhaust outflow from the combustion engine head is determined by the formula for the fill factor (8.2). Thus:

$$\dot{m} = \eta_V \cdot m_t, \quad (1)$$

where:

$\eta_V$  – fill factor,

$m_t$  – theoretical mass of charge fed to the cylinder,

$m_r$  – the actual mass of charge brought to the cylinder.

The theoretical mass flow of the fluid flowing under the given engine operating conditions is specified by the formula [1]:

$$\dot{m} = \frac{2 \cdot V_{SS} \cdot n \cdot \rho}{60000 \cdot \tau} \left[ \frac{\text{kg}}{\text{s}} \right], \quad (2)$$

where:

$V_{SS}$  – engine displacement volume [ $\text{dm}^3$ ],

$n$  – engine speed [rev/min],

$\rho$  – density [ $\text{kg}/\text{m}^3$ ],

$\tau$  – number of engine strokes.

The formula for the actual mass of charge brought to the cylinder takes the form:

$$\dot{m} = \eta_V \cdot \frac{2 \cdot V_{SS} \cdot n \cdot \rho}{60000 \cdot \tau} \left[ \frac{\text{kg}}{\text{s}} \right]. \quad (3)$$

Dividing both sides of the equation by density, we get the formula for the actual volume flow:

$$\dot{Q}_t = \eta_V \cdot \frac{2 \cdot V_{SS} \cdot n}{60000 \cdot \tau} \left[ \frac{\text{m}^3}{\text{s}} \right], \quad (4)$$

where:

$\dot{Q}_t$  – theoretical volume flow.

Subsequently, dividing the theoretical volume flow through the cross-sectional area of the wire results in obtaining the dependence on the flow velocity:

$$v = \frac{\dot{Q}_t}{A} \cdot 10^6 \left[ \frac{\text{m}}{\text{s}} \right]. \quad (5)$$

where:

$A$  – area of cross-sectional the conductor [mm<sup>2</sup>].

The engine data is taken from the manufacturer's catalogue [7]:

- $V_{SS} = 499 \text{ cm}^3 = 0.499 \text{ dm}^3$ ,
- $n = 11000 \text{ rpm}$ ,
- $\tau = 4$ ,
- $\eta_V = 0.9$ .

Having the engine data, the theoretical volume flow was determined:

$$\dot{Q}_t \approx 0.04 \text{ m}^3/\text{s}.$$

Then the cross-sectional area of the wire:

$$A = \frac{\pi d^2}{4} [\text{m}^2], \quad (5)$$

where:

$d$  – diameter of the wire,  $d = 44 \text{ mm}$ ,

you can estimate the speed of the exhaust gas:

$$v = 27 \text{ m/s}.$$

The exhaust gas temperature from the spark-ignition engine with methanol and the ignition timing of 25° is assumed to be 673 K [4]. The exhaust gas composition for the main shares is 71% nitrogen, 14% carbon dioxide, 13% water vapour and 2% oxygen [3]. The physical properties have been determined for the composition thus adopted:

- specific heat: image:  $\approx 1138.95 \text{ J}/(\text{kg}\cdot\text{K})$ ,
- dynamic viscosity:  $\approx 1.5795 \text{ kg}/(\text{m}\cdot\text{s})$ ,
- density:  $1.089 \text{ kg}/\text{m}^3$ .

Data was entered into the Fluent computational system and calculations were performed that had 2,100 iterations in order to achieve convergence to the exact solution at  $10^{-6}$ .

### Analysis of calculation results

The following is the pressure field in the exhaust duct: Fig. 1a – solution No. 1, Fig. 1b – solution No. 2. The analysis of the distribution of pressure values is presented below.

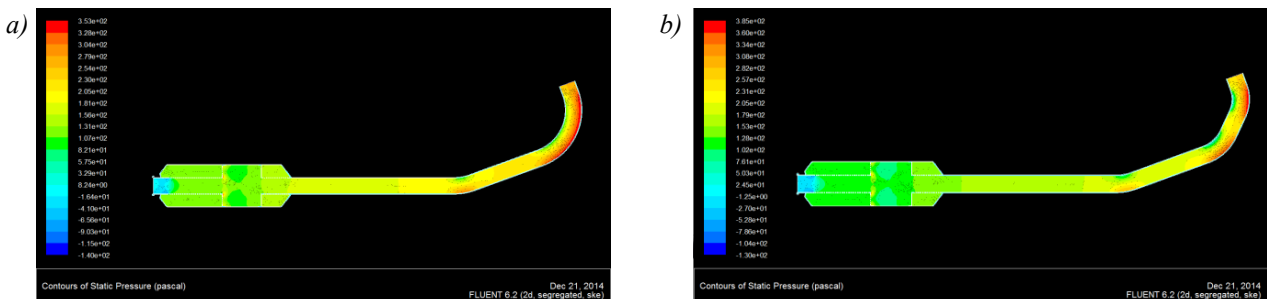


Fig. 1. Visualization of the relative pressure distribution in model 1 (a) and model 2 (b)

Located in Fig. 1, the inlet to the exhaust system is on the right. From the inlet to the exhaust pipe, we can observe the largest gradients of pressure in the entire exhaust system. Pressure gradients are caused by a change in the flow direction, which causes the change of kinetic energy accumulated in the accelerating gas column to the potential energy generated when encountering

an obstacle. In the case of gases, the increase in potential energy is manifested by the increase in pressure. The situation described above is the same as the flow resistance in fluid mechanics called local flow resistance. Thanks to numerical flow simulation you can in an engineering way, quantify the values of pressure differences for both solutions.

Solution No. 1 is characterized, on the entire length of the arc of elbow, by differences in pressure values ranging from 107 Pa to 353 Pa (Fig. 2).

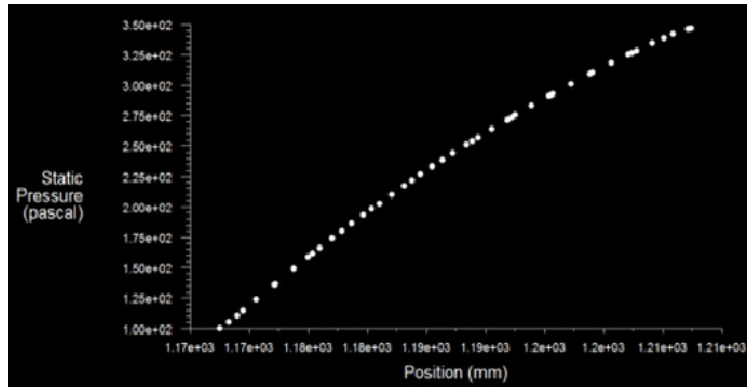


Fig. 2. Diagram showing the relative pressure in the cross-section of the arc in model 1

Following the direction of the flow, the relative pressure behind the arc is at 220 Pa. In the middle part of the muffler, the relative pressure value is in the range of 107-130 Pa, while at its outlet the value is about 8 Pa.

Solution No. 2 is characterized by a different course of change in pressure value. Starting the description from the inlet, i.e. from the right side of Fig. 1b, the exhaust gases overcome two smaller arcs, 45° each. The flow through the said bends, similarly as in solution No. 1, is subject to local losses observed in the form of a gradient of exhaust gas pressure values. Pressure values in the first of the bends range from 25 Pa to 385 Pa (Fig. 3).

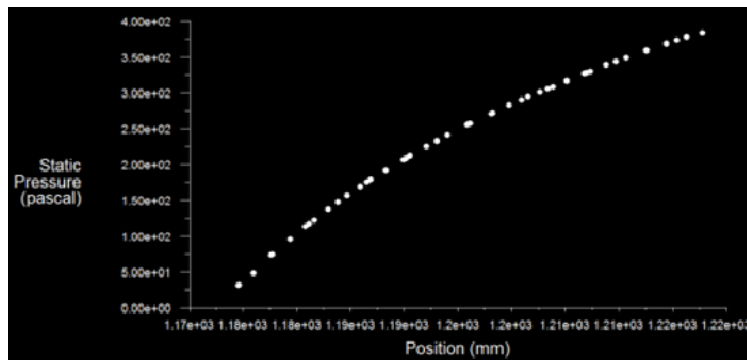


Fig. 3. Diagram showing the relative pressure in the cross-section of the first curve of model 2

However, when analysing pressure values in the direction of flow behind the first arc, the pressure in the straight section has a value of approximately 230 Pa. Moving the observation point further, in the second arc the relative pressure varies from 25 Pa to 350 Pa (Fig. 4).

When the exhaust gas flows through the arc area, the relative pressure of the exhaust gas reaches a value of approximately 200 Pa. Comparing the above-mentioned value to the analogous place in solution No. 1, the pressure was within 76-110 Pa. At the output, the pressure is at the ambient pressure level.

The flow through the base of the pressure field, described above, can be presented in the form of a velocity field. According to the flow continuity equation, local losses can also be observed in the form of velocity value gradients.

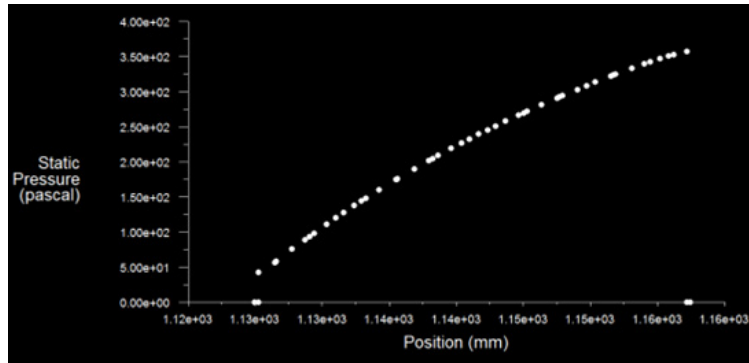


Fig. 4. Diagram showing the relative pressure in the cross-section of the second curve of model 2

Using engineering analysis, it is possible to quantify the size changes numerically and for solution No. 1, they will have values as in Fig. 5.

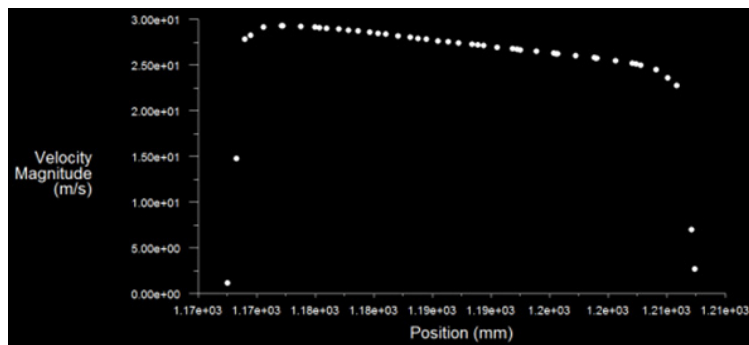


Fig. 5. Diagram showing the velocity distribution in the cross-section of the arc of model 1

On the inside of the curve, the exhaust velocity reaches 30 m/s, while on the outside it drops to 25 m/s. The difference in speed is therefore about 5 m/s. In this model, the speed at which exhaust gases leave the exhaust system is approx. 33 m/s (Fig. 6).

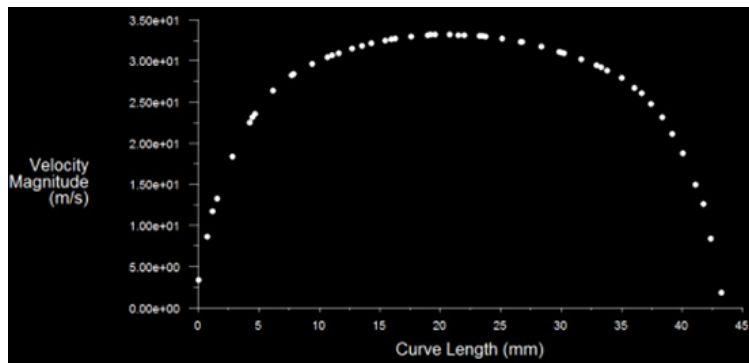


Fig. 6. Graph showing the exhaust velocity distribution at the outlet from the muffler of model 1

Solution No. 2 is characterized by the following course of velocity values: over the first curve, the velocity difference ranges from 32 m/s on the inside of the curve to the velocity of 22 m/s on the outside of the curve. (Fig. 7).

Analysing the flow further in the direction of flow, the flue gas moves at a speed of about 26 m/s and reaches the second curve.

The flow through the second curve can be characterized by velocities ranging from 28 m/s on the inside of the curve to 21 m/s on the outside of the curve. At the muffler outlet, the exhaust velocity reaches 32 m/s.

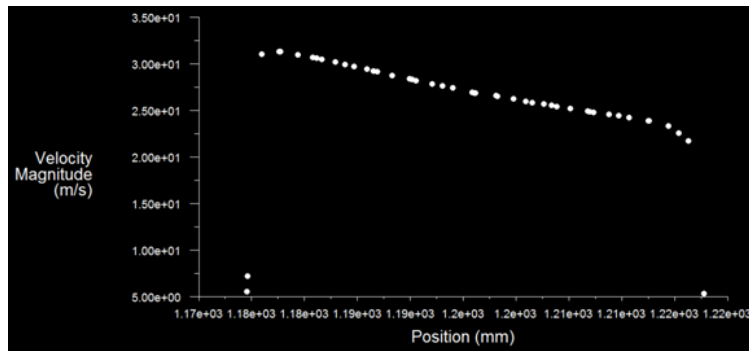


Fig. 7. Graph showing the velocity distribution in the cross-section of the curve of model 1

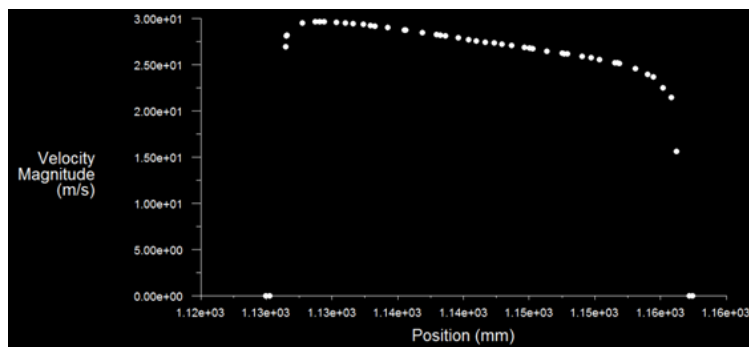


Fig. 8. Graph showing the exhaust velocity distribution in the cross-section of the second curve of model 2

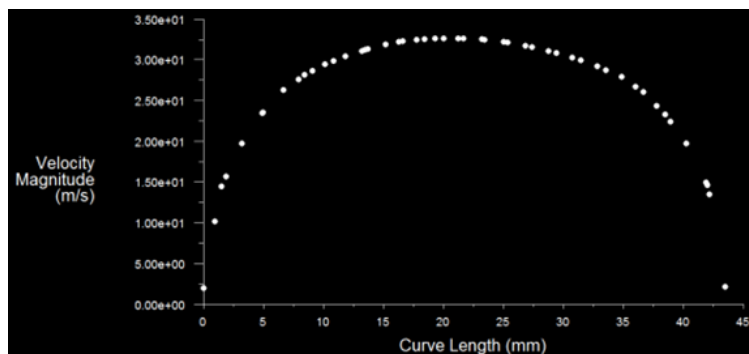


Fig. 9. Graph showing the exhaust velocity distribution at the muffler outlet of model 2

## 2.2. Conclusions

The analysis shows that solution No. 1, i.e. with one arc changing the direction of exhaust flow by  $90^\circ$ , is a better solution than solution number 2 because the flow resistance is smaller. Reading the value of the relative pressure at the inlet, which is approx. 270 Pa, it can be estimated that the value of local losses on the arc in this variant is 50 Pa. In turn, in the second variant, the pressure drop is equal to 70 Pa. Consequently, the overall pressure drop across the entire exhaust system is also smaller in the first solution.

In addition, in this design the cross-section area in the first arc is better used. The flow velocity field is more even. The difference in extreme speeds is 5 m/s, while in the competing solution the value is almost twice as high. As a result, the speed decrease is smaller, resulting in a 1 m/s higher exhaust velocity at the outlet than in the second variant. Although it may seem that this value is negligible, even such a difference can significantly affect the performance of the engine. This is particularly important in sports, where every second matters.

Our conclusions can be confronted with empirical formulas concerning local losses, which are contained in norm PN-76M-34034. The size of the local discharge coefficient for the arc can be

determined from the relationship:

$$\zeta = \left[ 0.131 + 1.847 \cdot \left( \frac{r}{R} \right)^{3.5} \right] \cdot \left( \frac{\phi}{90} \right) [-], \quad (5)$$

where:

$r$  – inner radius of the cable [mm],

$R$  – radius of the arc of the wire [mm],

$\phi$  – arc angle of the conductor [°].

For the first solution ( $r = 22$  mm,  $R = 120$  mm,  $\phi = 90^\circ$ ) the estimated value of the coefficient is 0.14. And for the second ( $r = 22$  mm,  $R = 70$  mm,  $\phi = 45^\circ$ ) is 0.16. As you can see, our conclusions were correct, because the empirical formulas show that the solution with two arches is characterized by a higher coefficient of local resistance.

Having local drag coefficients, we can determine whether the pressure loss amounts obtained using numerical methods, coincide with the values obtained using empirical formulas. Using the formula (9.9), it can be estimated that for the first exhaust system the pressure losses are 56 Pa and for the second 64 Pa. It can be seen that both methods give similar results.

### 3. Summary

Based on the example described above, you can see the utility of the tool, which is numerical flow analysis. In a relatively short time, we are able to obtain precise results of the parameters we are interested in without the need to carry out often expensive and time-consuming experimental tests. Convenient visualization of the obtained results enables a precise understanding of the device's operation and interdependencies between various factors. This is particularly important in studies of intake or exhaust systems of internal combustion engines, because the phenomena occurring in them are often complex and complicated, which makes it difficult to observe them on real models. In addition, the ability to immediately change the dimensions of the physical model significantly facilitates the work of engineers, because they can easily check the validity of their assumptions about changes aimed at improving the operation of a given device. In addition, the evaluation of the stationary flow and the determination of the flow discharge coefficient is a preliminary element to the gasodynamic analysis of the operation of a complete engine.

### References

- [1] Blair, G. P., *Design and simulation of four-stroke engines*, SAE. Warrendale, USA 1999.
- [2] Kmiotek, M., *Przegląd solverów numerycznych stosowanych w mechanice obliczeniowej*, Scientific Biuletyn of Chełm, Chełm 2008.
- [3] *Motor Vehicle Exhaust Emissions*, Volkswagen AG Wolfsburg.
- [4] Nirmala Devi, E., et al., *Int. Journal of Engineering Research and Applications*, Vol. 3, Iss. 6, pp. 1351-1354, 2013.
- [5] Fédération Internationale de Motocyclisme, *Technical rules for track racing*, [http://www.pzm.pl/pliki/zg/zuzel/2014/regulamin/2014\\_ccp\\_technical\\_rules\\_final.pdf](http://www.pzm.pl/pliki/zg/zuzel/2014/regulamin/2014_ccp_technical_rules_final.pdf).
- [6] Górnjak, A., Michałowski, R., Tkaczyk, M., *Computational fluid dynamic simulation of a combustion engine powered by compressible natural gas*, *Polish Journal of Environmental Studies*, Vol. 21, No. 5A, pp. 85-89, 2012.
- [7] Speedway Catalog, [http://www.gmengines.net/gm\\_500\\_product\\_info.htm](http://www.gmengines.net/gm_500_product_info.htm).

*Manuscript received 19 July 2018; approved for printing 23 October 2018*